



Contents lists available at ScienceDirect

Science of the Total Environment

journal homepage: www.elsevier.com/locate/scitotenv



The Carbon-Capture Efficiency of Natural Water Alkalinization: Implications For Enhanced weathering

Matteo B. Bertagni^{a,*}, Amilcare Porporato^{a,b}

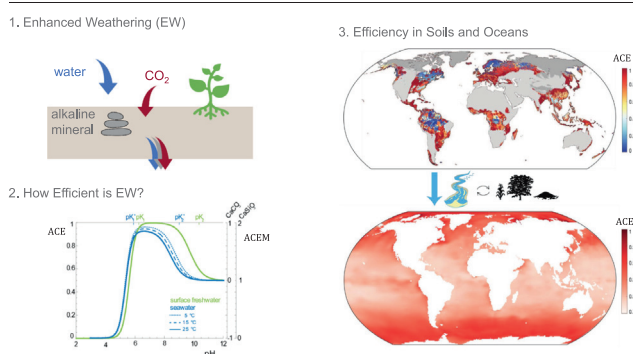
^a The High Meadows Environmental Institute, Princeton University, Princeton, NJ 08544, USA

^b Department of Civil and Environmental Engineering, Princeton University, Princeton, NJ 08544, USA

HIGHLIGHTS

- We assess the carbon-capture efficiency of alkaline mineral dissolution in natural waters
- We investigate the strong dependence of the carbon-capture efficiency on the water chemistry
- In the world topsoil, the efficiency ranges from 0 to 100 % with an important trade-off between carbon-capture efficiency and enhanced chemical dissolution
- In the surface ocean, the efficiency is around 80 % with a latitudinal pattern induced by seawater temperature and salinity

GRAPHICAL ABSTRACT



ARTICLE INFO

Editor: Daniel Alessi

Keywords:

Enhanced weathering
Negative-emission technology
Alkalinization
Natural waters
Soils
Ocean

ABSTRACT

Enhanced weathering (EW) is a promising negative-emission technology that artificially accelerates the dissolution of natural minerals, promotes biomass growth, and alleviates the acidification of soils and natural waters. EW aims to increase the alkalinity of natural waters (alkalinization) to promote a transfer of CO₂ from the atmosphere to the water. Here we provide a quantification of the alkalinization carbon-capture efficiency (ACE) as a function of the water chemistry. ACE can be used for any alkaline mineral in various natural waters. We show that ACE strongly depends on the water pH, with a sharp transition from minimum to maximum in a narrow interval of pH values. We also quantify ACE in three compartments of the land-to-ocean aquatic continuum: the world topsoils, the lakes of an acid-sensitive area, and the global surface ocean. The results reveal that the efficiency of terrestrial EW varies markedly, from 0 to 100 %, with a significant trade-off in acidic conditions between carbon-capture efficiency and enhanced chemical dissolution. The efficiency is more stable in the ocean, with a typical value of around 80 % and a latitudinal pattern driven by differences in seawater temperature and salinity. Our results point to the importance of an integrated hydrological and biogeochemical theory to assess the fate of the weathering products across the aquatic continuum from land to ocean.

1. Introduction

Among the several strategies that are being developed to sequester atmospheric CO₂ (Griscom et al., 2017; Pacala et al., 2018), Enhanced Weathering (EW) has gained attention as a promising geoeengineering

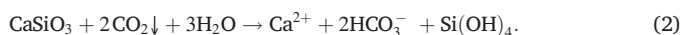
solution with large potential for CO₂ removal and limited technological requirement (Beerling et al., 2020; Köhler et al., 2010; Calabrese et al., 2022; Hartmann et al., 2013). EW consists in spreading finely ground rocks rich in alkaline minerals in environments where the mineral dissolution might be favored, as in the acidic soils of croplands and forests (Hartmann et al., 2013; Calabrese and Porporato, 2020). In addition to sequestering CO₂, the mineral dissolution provides important co-benefits, like counteracting soil acidification and promoting biomass growth due to the addition of biological macronutrients such as calcium (Ca), magnesium (Mg) and

* Corresponding author.

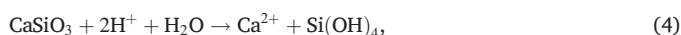
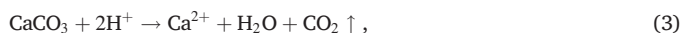
E-mail addresses: matteobb@princeton.edu (M.B. Bertagni), aporpora@princeton.edu (A. Porporato).

phosphorus (P) (Beerling et al., 2018; Goll et al., 2021). Part of the mineral dissolution products are then transported by the hydrologic cycle to surface freshwaters and, eventually, the ocean, mitigating ocean acidification and stably sequestering atmospheric CO₂ for geological timescales (Renforth and Henderson, 2017). A potential negative side effect of EW is the release of heavy metals like nickel (Ni) and chromium (Cr) that can be present in silicate rocks (Haque et al., 2020).

The negative-emission potential of EW relies on increasing the alkalinity (alkalinization) of natural waters through mineral dissolution, thereby promoting a transfer of CO₂ from the atmosphere to the water. The efficiency of such a CO₂ transfer strongly depends on the water-chemistry conditions where the alkalinization occurs. For example, at neutral pH's, the dissolution of calcium carbonate (CaCO₃) and wollastonite (CaSiO₃) promotes the formation of bicarbonates (HCO₃⁻) according to the well-known reactions (Hartmann et al., 2013)



Differently, in the acidic soils of forest and fertilized crops, carbonate formation is hampered (Hartmann et al., 2013; West and McBride, 2005) and the mineral dissolution reactions can be summarized as in



where Eq. (3) shows that CaCO₃ dissolution in acidic conditions releases CO₂ to the atmosphere. The loss of carbon-capture efficiency implied by (3) and (4) has long been recognized (Hartmann et al., 2013; West and McBride, 2005) and is the reason why the Intergovernmental Panel on Climate Change (IPCC) conservatively assumes that all carbon involved in agricultural liming is released to the atmosphere (Klein et al., 2006).

More generally, the two cases represented by (1)–(2) and (3)–(4) are only two end members along a continuum of water-chemistry conditions that correspond to different alkalinization carbon-capture efficiencies. Notwithstanding its importance, a detailed quantification of the alkalinization efficiency along this continuum is currently lacking. This has important consequences for the modeling of the carbon cycle as affected by natural and artificially enhanced mineral weathering. For example, it is actually unknown whether agricultural liming is a global source or sink of atmospheric CO₂ (Klein et al., 2006; Hamilton et al., 2007; Wang et al., 2021). Furthermore, it is currently unclear how to quantify the carbon capture-efficiency of EW applications as a function of the chemical condition of the water solution both at the site of dissolution and along the hydrologic pathway where the mineral dissolution cations are transported.

To fill this gap, here we derive an analytical factor that quantifies the variation in the Dissolved Inorganic Carbon (DIC) in the water in response to a small increase in water alkalinity (Alk). We refer to this factor as the Alkalinization Carbon-capture Efficiency (ACE). We show that ACE can be used to: i) quantify the amount of CO₂ captured per unit of alkalinity added as a function of the water chemistry, either at the site of dissolution or at the hydrological site where the alkalinity is transported; ii) quantify the carbon-capture efficiency of any specific mineral, in turn indicated as ACEM; iii) generalize the dissolution reactions (1)–(4) to account for the continuum of the water-chemistry conditions (Appendix B).

Using ACE as a theoretical benchmark to assess EW efficiency, we present evaluations of ACE across three main compartments of the aquatic continuum from land to ocean, namely the world topsoils, the freshwater lakes of an acid-sensitive region, and the global surface ocean. The results highlight an important trade-off of terrestrial EW in acidic conditions between enhanced mineral dissolution and inefficient carbon capture. The efficiency is more stable once the alkalinity reaches the ocean. We also

discuss how the hydrologic connectivity between these compartments through groundwater and rivers remains one of the key open questions that needs to be addressed to better define what fraction of the mineral cations are transported along the hydrological cycle and what are the timescales involved.

The paper is structured as follows: Section 2 defines the generic form of the alkalinization carbon-capture efficiency (ACE) and the specific efficiency of any mineral (ACEM); Section 3 explores the influence of typical conditions of natural waters on ACE; Section 4 assess the influence of large alkalinity perturbations; Section 5 presents and discusses the values of ACE in the world topsoils, the lakes of an acid-sensitive region and the surface ocean; Section 6 summarizes our main findings and the hydrological and biogeochemical challenges for future research.

2. Theoretical considerations

We start by defining the general expression of the alkalinization carbon-capture efficiency (ACE) as well as the specific efficiency for any mineral (ACEM). The derivation of ACE is reported in Appendix A.

2.1. Alkalinization Carbon-capture Efficiency (ACE)

In a water solution in equilibrium with the atmosphere, the knowledge of one between the water alkalinity and the water pH is sufficient to define the concentrations of the aqueous carbonate species (Fig. A.6). A variation in water alkalinity (Alk) by mineral dissolution affects the water pH and the amount of dissolved inorganic carbon (DIC) sequestered in the water. As a result, the carbon-capture efficiency of alkalinization can be defined as the variation of [DIC] driven by a small change in [Alk], where [·] indicate molar concentration (M). ACE can be expressed as a function of the partial pressure of carbon dioxide in the air (*p*_{CO₂}) and the water pH (pH = − Log [H⁺]) as in

$$\text{ACE} = \frac{d[\text{DIC}]}{d[\text{Alk}]} = \frac{K_1 K_H p_{\text{CO}_2} ([\text{H}^+] + 2K_2)}{k p_{\text{CO}_2} + [\text{H}^+] (K_1 K_H p_{\text{CO}_2} + K_w) + [\text{H}^+]^3 (1 + f_B)}, \quad (5)$$

where *K*₁ and *K*₂ are the first and second dissociation constants of carbonic acid, respectively, *K*_H is Henry's solubility constant of CO₂, *k* = 4*K*₁*K*₂*K*_H, and *f*_B is a term indicating the influence of borates in seawater (Appendix A). By quantifying the variation of [DIC] due to a small change in [Alk], ACE provides an objective measure of the sensitivity of the concentration of inorganic carbon in water to alkalinity. Conveniently, ACE varies between 0, when the alkalinity variation does not affect the amount of DIC in the water, and 1, when the alkalinity increment corresponds to an equal increment of DIC. Moreover, the definition of ACE is valid for any biogeochemical process that affects the water alkalinity (e.g., mineral dissolution or precipitation, nutrients uptake by biota, etc.). More broadly, many factors that are obtained as the ratio of differentials of two variables of the water-air system have been proposed in the oceanographic literature so far (Frankignoulle, 1994; Egleston et al., 2010; Humphreys et al., 2018; Middelburg et al., 2020), e.g., the well-known Revelle factor, which is the ratio of the differentials of *p*_{CO₂} and [DIC] (Revelle and Suess, 1957). These factors are of extreme interest to oceanographers and climate-change scientists, as they serve as rigorous tools to evaluate the response of the ocean to natural and human-induced changes. The factor (5) was previously used to evaluate the response of the ocean carbonate system to an input of acid rain (Frankignoulle, 1994). Because of the recent interest in terrestrial EW, here we use ACE to quantify the efficiency of carbon capture by alkaline mineral dissolution both in seawater and freshwater, investigating how the different chemical conditions of soil and surface freshwaters worldwide may affect the carbon-capture efficiency.

2.2. ACE of a Mineral (ACEM)

Based on the definition of ACE, we define the carbon-capture efficiency of a given mineral (ACEM) as the CO₂ captured in the aqueous solution per molecule of mineral dissolved. In formula,

$$ACEM = n_M ACE - C_M, \quad (6)$$

where the subscript M indicates that the parameter depends on the mineral considered (see Table 1); C_M is the number of carbon atoms contained in the mineral molecule; and n_M is the increase in alkalinity caused by a molar increment in the amount of dissolved mineral. To evaluate n_M, it is convenient to express the alkalinity in terms of only species that are conservative to changes in pressure, temperature, and pH (Zeebe and Wolf-Gladrow, 2001; Wolf-Gladrow et al., 2007).

$$[Alk] = 2[Ca^{2+}] + 2[Mg^{2+}] + [K^+] + [Na^+] - 2[SO_4^{2-}] - 2[NO_3^-] - [Cl^-] \pm \dots, \quad (7)$$

where the ellipses indicate the possible presence of other conservative cations (+) or anions (−) in the water solution. From (7), it is evident that the dissolution of a molar unit of CaCO₃ or CaSiO₃ increases water alkalinity by 2 M units as Ca²⁺ is added into the water, i.e., n_{CaCO₃} = n_{CaSiO₃} = 2.

Using the definition of ACEM, we can generalize the mineral dissolution reactions, like (1)–(4) for CaCO₃ and CaSiO₃, to account for the different carbon-capture efficiencies as a function of the water chemistry. This is shown and discussed in detail in Appendix B.

It is important to bear in mind that ACEM quantifies the carbon capture that follows the mineral dissolution, but clearly does not address the time-scales at which the dissolution takes place. These vary greatly as a function of the mineral and the environment considered. For example, artificial minerals (e.g., Ca(OH)₂) rapidly dissolve in every natural water, offering a great potential of rapid carbon sequestration (Renforth, 2019), while silicate minerals (e.g., CaSiO₃) need an environment that enhances the very slow dissolution rates to be effective in timescale that are useful to climate-change mitigation (Hartmann et al., 2013).

3. Influence of environmental conditions

Here we explore the influences on ACE of the air-water system parameters (pH, p_{CO₂} and temperature) for typical conditions of soil water, freshwater, and seawater.

3.1. Influence of pH and temperature for freshwater and seawater

The factor ACE, and consequently also the efficiency for the different minerals, strongly depend on the water pH. In particular, as shown in Fig. 1a, ACE undergoes a sharp transition between values close to zero and a maximum (ACE ≈ 1 for freshwater and ACE ≈ 0.9 for seawater) in the pH range 4.5 to 6.5, which corresponds to the transition between mineral-acidic and alkaline waters (Fig. A.6).

ACE is basically zero at pH < 5 since, at these pH's, the carbonate ions (HCO₃[−] and CO₃^{2−}) do not form (see also Fig. A.6 and C.7). On the contrary, ACE is maximized when the increase in alkalinity is associated with an increment in the concentration of bicarbonate ions HCO₃[−] (i.e., for pH >

pK₁). This maximum of ACE is rather flat and forms a plateau, which is broader for freshwater than seawater. At even higher pH, ACE decays again to ≈ 0.5 (at pH > pK₂) as bicarbonates (HCO₃[−]) are substituted by carbonates (CO₃^{2−}).

Even though the trend of ACE is qualitatively similar for seawater and freshwater, there are substantial quantitative differences. Regarding the maximum of ACE, while in freshwater the variation in alkalinity may be completely associated with the carbonate buffer (max of ACE ≈ 1), in seawater the variation in alkalinity is partially associated with the borate buffer (max of ACE < 1). This effect is stronger at higher temperatures because the CO₂ solubility decreases and the ratio of total borates (conservative to temperature variation) to DIC (non-conservative) increases.

The difference in the plateau width of the maximum of ACE is instead due to the different dissociation constants for carbonic acid in freshwater pK₁, pK₂, i.e., thermodynamic constants in the approximation of diluted waters, and seawater pK₁^{*}, pK₂^{*}, i.e., stoichiometric constants accounting for salinity. Specifically, since pK₂^{*} < pK₂, which indicates that seawater has a much higher concentration of CO₃^{2−} than freshwater at the same pH, the decay of ACE from the plateau occurs at lower pH values for seawater. This is an important factor in reducing the carbon capture efficiency in the ocean and provides an analytical quantification of the loss of efficiency in seawater that was previously pointed out (Köhler et al., 2010; Khesghi, 1995).

3.2. Influence of p_{CO₂} and implications for EW in soils

Beside pH and temperature, the other parameter affecting ACE is the p_{CO₂}, i.e., the concentration of CO₂ in the air. Some of the largest ranges of p_{CO₂} are found in soils, where, due to biotic respiration, p_{CO₂} can be much higher than the typical atmospheric values. This is one of the reasons soils are considered as a convenient environment for EW (Hartmann et al., 2013).

Fig. 1b shows a 2D plot of ACE as a function of pH and p_{CO₂}. The p_{CO₂} weakly affects the pH region of transition between the ACE minimum and maximum, which is around the transition between alkaline and acidic waters, i.e., pH₀. To an increase in p_{CO₂} there corresponds a shift in the lower limit of the pH interval where ACE is maximized. Recalling that a lower pH would favor the mineral weathering, these results suggest that the soil is a very efficient environment for EW. Furthermore, as shown in the Supplementary (Fig. S2), the possible presence of other weak acids or bases in the soil water solution (e.g., phosphoric acid) has only a minor effect on ACE.

However, it is important to stress that the carbon capture efficiency of the alkaline cations is bound to their permanence in the soil water solution, which, in the highly dynamic soil environment, may be altered by biotic and abiotic processes such as plant uptake and adsorption by colloids (Calabrese et al., 2022; Amann et al., 2020).

4. Influence of alkalinity perturbation

The definition of ACE is exact for a small perturbation of alkalinity (d[DIC]/d[Alk]) and is likely useful for most environmental purposes, wherein large variations in the water chemistry are undesired to minimize the impact on the aquatic biota. Nonetheless, for EW applications in very acidic soils, where a large increase in pH can be actively sought, it is worth comparing how the carbon capture efficiency varies with a large alkalinity perturbation (Δ[DIC]/Δ[Alk]).

Since for a natural water in equilibrium with the atmosphere, the knowledge of one among Alk, DIC and pH is sufficient to define the others, it is possible to evaluate the difference in DIC (Δ[DIC]) and pH (ΔpH) that follows an alkalinity addition (Δ[Alk]) for a given initial condition. This can be done numerically using the equations reported in Appendix A. Fig. 2 shows the results for a freshwater. The gray-shaded region marks where Δ[DIC]/Δ[Alk] deviates from ACE. The lower edge of this region hence defines, as a function of the initial pH, how large the alkalinity perturbation can be for ACE definition to hold.

Fig. 2 shows that ACE is a very good approximation of Δ[DIC]/Δ[Alk] even for large alkalinity additions for most of the initial pH values. The only exception is when the water pH is around pH₀, namely in the transition

Table 1

ACEM and related parameters for some common natural minerals and artificial materials. ACEM is reported as [minimum, maximum].

Mineral	n	C	ACEM
CaSiO ₃	2	0	[0,2]
Mg ₂ SiO ₄ , Fe ₂ SiO ₄	4	0	[0,4]
CaCO ₃ , MgCO ₃	2	1	[−1,1]
CaMg(CO ₃) ₂	4	2	[−2,2]
Ca(OH) ₂ , Mg(OH) ₂	2	0	[0,2]
CaO, MgO	2	0	[0,2]

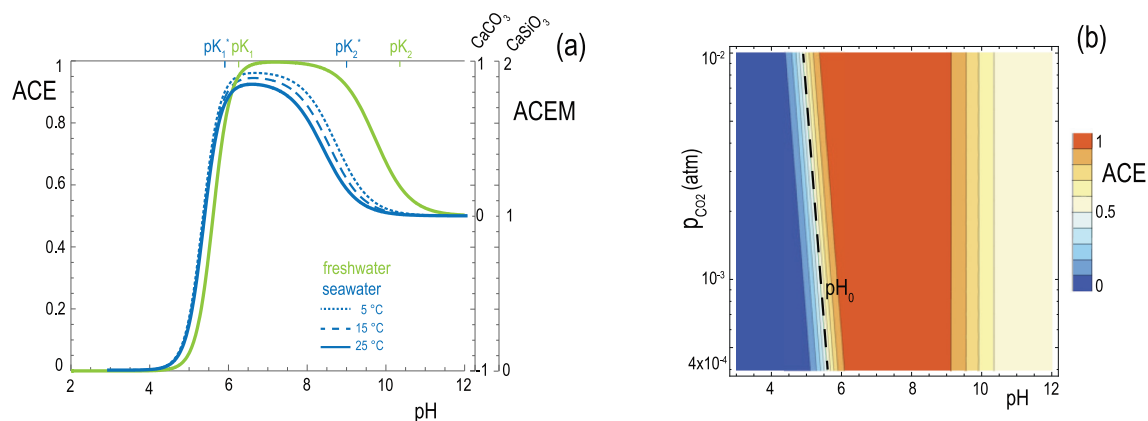


Fig. 1. Alkalization carbon-capture efficiency (ACE) as a function of the water chemistry. (a) ACE and ACEM for CaCO_3 and CaSiO_3 , as a function of pH for freshwater (green) and seawater (light blue) in equilibrium with the atmosphere ($p_{\text{CO}_2} = 4 \cdot 10^{-4}$ atm). Temperature effect for freshwater is negligible (not shown). pK_1 , pK_2 and pK_1^* , pK_2^* are the dissociation constants of carbonic acid for freshwater and seawater, respectively (labelled in the upper axis for $T = 25^\circ\text{C}$ and average ocean salinity 35 ‰). (b) Contour plot of the factor ACE in the plane $\{pH, p_{\text{CO}_2}\}$ for a soil freshwater. The black dashed line (pH_0) separates alkaline and mineral-acidic waters (i.e., $[\text{Alk}] = 0$).

region between mineral acidic and alkaline waters. In this case, a relatively small alkalinity addition (10 to 100 μM_{eq}) is sufficient to shift the water chemistry from the conditions that minimize ACE to the ones that maximize it (following the trend in Fig. 1a). In other words, a finite alkalinity addition to an initially slightly mineral-acidic water increases the water pH considerably, leading to conditions that are favorable to carbonate formation and therefore $\Delta[\text{DIC}]/\Delta[\text{Alk}] > \text{ACE}$. Besides this exception, the fact that ACE is generally a good estimate of $\Delta[\text{DIC}]/\Delta[\text{Alk}]$ supports ACE applicability for most practical purposes. Hence, in the following section, we use ACE to evaluate the efficiency of natural waters' alkalization for some compartments of the land-to-ocean aquatic continuum.

5. ACE in soils, lakes, and oceans

Some dissolution products are taken up by ecosystems in the terrestrial site of mineral application, while some are transported by the hydrological

cycle to surface waters and, eventually, the ocean. The timescale and intensity of this transport are open questions that critically depend on the hydrologic connectivity of the mineral application site to surface water bodies across the watersheds and the fluvial network. Here we adopt a simplified approach where we provide evaluations of ACE for three main compartments in the hydrologic continuum, namely topsoils, lakes and the surface ocean, wherein near equilibrium conditions can be reasonably assumed. These first assessments of EW efficiency may serve as benchmarks for subsequent, more detailed analyses that include hydrologic connectivity and biogeochemical processes.

Specifically, we present a global analysis of topsoils, where we combine the evaluation of the carbon capture efficiency with considerations on mineral dissolution kinetics; a local analysis for the freshwater lakes of an acid-sensitive region; and a global analysis of the surface ocean.

5.1. A global topsoil analysis

We first evaluate the global pattern of ACE in the world topsoils and analyze the influence of the hydroclimatic forcings on the mineral dissolution rates. Used data and methods are reported in Appendix C. Because a sufficiently wet and warm soil environment is required for the weathering of minerals, silicates in particular, mostly temperate-humid and tropical regions are suitable for EW applications (Hartmann et al., 2013; Calabrese and Porporato, 2020). Within these regions, the results show that ACE varies greatly (Fig. 3a). It is maximized in mildly acidic or alkaline areas (e.g., Central Europe, Eastern Asia) and minimized in very acidic soils (e.g., central Amazon, Northeastern United States).

This pattern of carbon-capture efficiency per unit of alkalinity is opposite to the tendency of the minerals to dissolve. That is, in the acidic soils where $\text{ACE} = 0$, the mineral dissolution rates are much higher than in the alkaline soils where $\text{ACE} = 1$ (Fig. 3b). This results in an important trade-off between carbon capture efficiency and enhanced chemical dissolution. Since temperature also affects the dissolution rate, tropical acid soils are the most effective environment in terms of enhanced mineral dissolution. In these soils, however, not only the carbon capture efficiency in the soil water is hampered by the low pH values, but also a good fraction of the mineral cations may be lost to ecosystem uptake due to the high biomass density and the relative deficiency of alkaline nutrients.

These results suggest that the efficiency of EW in the acidic soils, where mineral dissolution rates are maximized, may be constrained to three possible scenarios: i) the EW application leads to a large alkalinity perturbation rising the soil water pH to values that are favorable to carbonate formation, as shown in Fig. 2; ii) the ecosystem uptake of alkaline nutrients mitigates a nutrient deficiency and promotes additional biomass growth, increasing

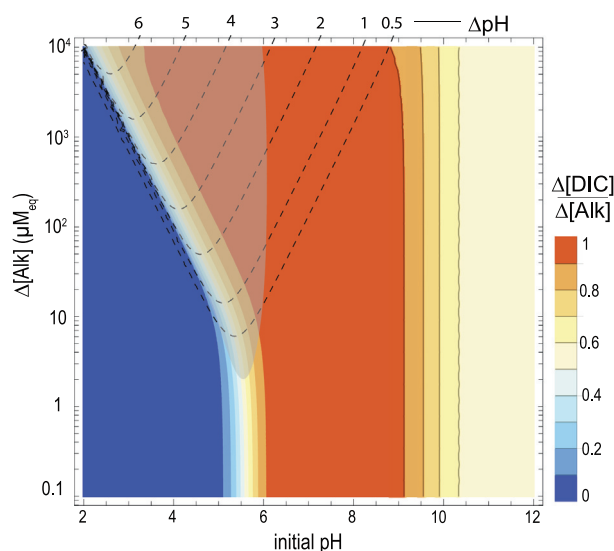


Fig. 2. Carbon-capture efficiency of a large alkalinity perturbation ($\Delta[\text{DIC}]/\Delta[\text{Alk}]$) as a function of the initial pH and the amount of added alkalinity (freshwater in equilibrium with the atmosphere at standard conditions). Dashed contours define the increase in the pH (ΔpH) caused by the alkalinity addition. The gray-shaded area marks where $\Delta[\text{DIC}]/\Delta[\text{Alk}]$ deviates from ACE, specifically $\Delta[\text{DIC}]/\Delta[\text{Alk}] - \text{ACE} > 0.1$.

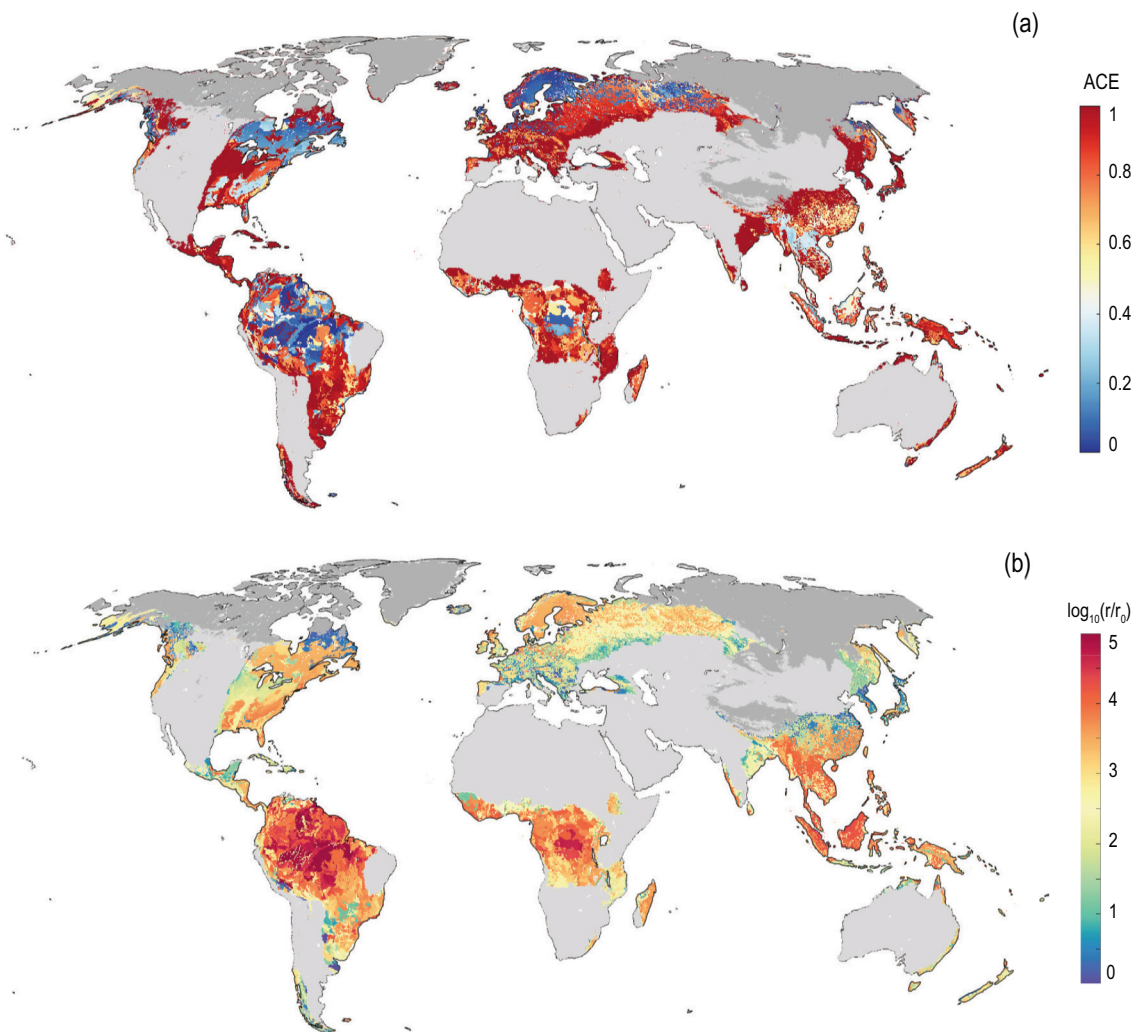


Fig. 3. Alkalinization carbon-capture efficiency (a) and hydroclimatic-driven scaling of the mineral dissolution rates (b) in the world topsoils (0–30 cm). Dark and light gray regions are respectively too cold (average temperature below 0 °C) or too arid (aridity index above 3 (Calabrese and Porporato, 2020)) for EW applications. r/r_0 shows the scaling of a mineral dissolution rate with soil moisture, pH, and temperature (details in Appendix C).

the biotic carbon stock of forests (Taylor et al., 2021) or the yield of crops (Kelland et al., 2020); iii) the mineral cations are transported by the hydrological cycle from the acidic soil water to another water solution, where they can actively transfer atmospheric CO_2 to the water.

This raises the question regarding the fraction of the mineral dissolution products that is hydrologically transported, as well as of the timescales involved in this transport. Answering these questions is complicated by the partial decoupling of the cation transport and the hydrological cycle, due to ecosystem uptake and soil adsorption (Calabrese et al., 2022). In this perspective, a recent one-year mesocosm experiment has shown that only a minor fraction of the Mg^{2+} released by olivine dissolution actually leached from the root zone (Amann et al., 2020). Since biotic and abiotic uptake could potentially affect the mineral cation transport from the root zone to the ocean, through aquifers, riparian areas and the entire river network, further theoretical and field research is needed to assess the fate of mineral cations and their related carbon-capture efficiency in view of the couplings between hydrological and biogeochemical cycles.

5.2. Acid-sensitive lakes

Lakes are both an intermediate step in the transport of mineral cations from the soils to the ocean and a direct target of EW (mostly CaCO_3) to counteract their acidification (Mant et al., 2013; Menz and Seip, 2004). We consider here the lakes in the American Northern Atlantic coast,

which are still in a recovering phase from past natural (i.e., organic acids) and anthropic (i.e., acid rains) acidification (Clair et al., 2011). These water bodies have been considered as potential candidates for EW applications (Sterling et al., 2014).

To highlight how the EW solution could change the dissolved inorganic carbon in these types of lakes, we calculated ACE for 156 lakes in this region assuming a small alkalinity variation and long-term equilibrium with the atmosphere, i.e., neglecting possible seasonal fluctuations of the CO_2 saturation state. Since we do not consider the organic buffer of the lakes, the ACE presented here is only an upper bound for the actual efficiency of the mineral cations. The results, shown in Fig. 4, indicate how the different lake pH's drive the carbon capture efficiency. In lakes with lower pH, the increase in alkalinity due to mineral cations does not promote any carbon capture in the lake water, implying that for carbonate minerals (e.g., CaCO_3), there would be a loss of carbon toward the atmosphere as $\text{ACE}_{\text{CaCO}_3} = -1$ from (6). To the purpose of climate mitigation, therefore, non-carbonate minerals should be preferred, but challenges persist on the slow dissolution of silicate minerals and the extremely fast dissolution of artificial materials (e.g., slack lime), which can cause burst in the water pH that are harmful to the aquatic biota. Regarding the residence time of the mineral nutrients in lakes, this crucially depends on the lake hydrologic connectivity to the stream network and the groundwater. Usually, there is a positive correlation between the water and the nutrient residence times, e.g., both residence times decrease with increasing hydrologic

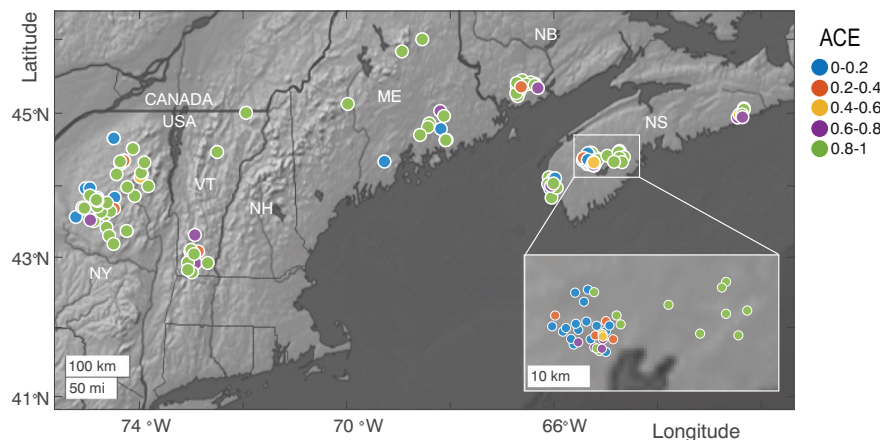


Fig. 4. Evaluation of ACE for 156 lakes in the acid-sensitive Atlantic region between the USA and Canada. pH values (2010–2017 averaged) have been obtained from the Long-Term Monitoring (LTM) EPA program for US lakes (EPA, 2021) and the Acid Sensitive Lakes Study for the Canada Lakes (Clair et al., 2011). $p_{\text{CO}_2} = 4 \cdot 10^{-4}$ atm, $T = 10^\circ\text{C}$.

connectivity of the lake. However, the high biological activity of some lakes can favor a biogeochemical recycling of the mineral cations that limits their downstream transport (Covino, 2017). This calls for further analyses that couple physical and biogeochemical controls on the fate of the mineral dissolution products in lentic systems.

5.3. Surface ocean

The ocean absorbs around a third of the anthropogenic CO_2 emissions, with a related 0.1 reduction in pH since preindustrial times which raises serious concerns for marine biology (Gattuso and Hansson, 2011; Gruber et al., 2019). The alkalization of the ocean by mineral dissolution would counteract such a trend and, at the same time, increase the CO_2 sequestration potential of the ocean, which is stable for geological timescales (≈ 1000 kyr, (Renforth and Henderson, 2017)). For example, direct local injections of alkalinity are being evaluated as a way to protect the Great Barrier Reef from acidification (Mongin et al., 2021).

As previously pointed out (Köhler et al., 2010), due to the ocean chemistry and in particular to the relatively high ratio of carbonate to bicarbonates, the carbon-capture efficiency of the mineral cations never reaches unity (Fig. 1a) and $\text{ACE} \approx 0.83$ for average conditions of seawater temperature (20°C), salinity (35 ‰) and pH (≈ 8.1). To further investigate the spatial pattern of the efficiency, we calculated the global distribution of ACE in the surface ocean.

The results, shown in Fig. 5, outline a latitudinal trend for ACE that is induced by differences in temperature and salinity. In particular, colder and fresher waters in arctic and antarctic latitudes favor the carbon capture efficiency ($\text{ACE} \approx 0.9$), compared to warmer and saltier waters in tropical and temperate latitudes ($\text{ACE} \approx 0.8$). This difference in efficiency results from the combined effects of higher CO_2 solubility at lower temperatures, and lower ratio of carbonate to bicarbonates in fresher waters (i.e., higher value of pK_2^*). An average value of $\text{ACE} \approx 0.8$ can be used as a reference for EW applications in tropical and temperate latitudes, where the mineral dissolution is favored by the higher temperatures.

6. Discussion and conclusions

The theoretical quantification of the carbon-capture efficiency of water alkalization (ACE) as a function of the water chemistry is a critical step to evaluate the potential of EW in soils and surface waters. The spectrum of applications covers any soluble alkaline mineral or material (ACEM) in a variety of natural waters.

The results have pointed out the strong dependence of ACE on the water pH (Fig. 1). In particular, ACE is minimum in acidic waters ($\text{pH} < 5$), and is maximum in alkaline waters where the formation of HCO_3^- is favored. In the sharp transition from minimum to maximum, ACE is very sensitive to variations of freshwater pH, which within the range 5 to 6 changes the ACE from 0.05 to 0.85. In this transition range, however, a relatively

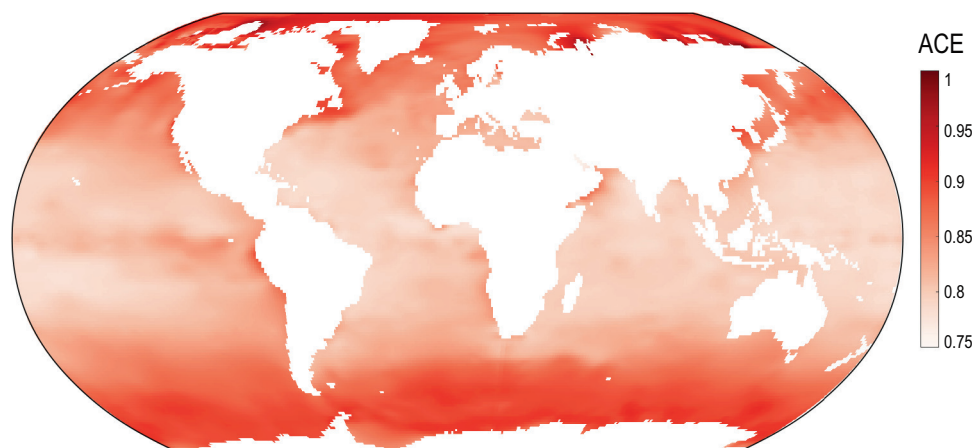


Fig. 5. Map of ACE in the surface ocean (30 m). Climatology data of DIC and Alk (1×1), which have been converted to p_{CO_2} and pH through CO2SYM software (Lewis and Wallace, 1998), are from the GLODAP project (Olsen et al., 2019; Olsen et al., 2020); temperature and salinity data (2005–2017 averaged) are from the World Ocean Atlas (Locarnini et al., 2018; Zweng et al., 2019).

small alkalinity addition ($\approx 100 \mu\text{M}_{\text{eq}}$) is sufficient to increase the water pH to values that are favorable to carbonate formation (Fig. 2).

ACE variability implies that EW may produce very different results in terms of carbon capture depending on the water conditions where the minerals are dissolved (Fig. 3a and 4). In particular, regarding terrestrial EW in the acidic soils where the mineral dissolution rates are usually maximized, there is an important trade-off between carbon capture efficiency and enhanced mineral dissolution (Fig. 3). To be efficient in acidic soils, EW should either promote a large pH variation that leads to carbonate formation, or increase the biotic carbon stock by favoring additional biomass growth. Alternatively, the efficiency of EW in these soils may be constrained to the transport of the mineral dissolution cations to the ocean, where the efficiency is more stable ranging from 0.75 to 0.9 depending on seawater temperature and salinity (Fig. 5). In particular, the carbon capture efficiency is lower in tropical and temperate latitudes (≈ 0.8) than in polar latitudes (≈ 0.9).

Assessing what fraction of the mineral dissolution products would be transported from soils to the ocean, and with which timescales, is not trivial. From the root zone to the ocean, through watersheds and the river network, several abiotic (e.g., soil adsorption) and biotic (e.g., plant uptake) processes could partially decouple the mineral cation transport and the hydrological cycle. Combining these considerations with ACE for soils and the surface ocean will help assess the efficiency trade-off between terrestrial enhanced weathering, where the mineral dissolution rates are higher but the carbon capture efficiency is less stable, and the direct ocean alkalization, where the dissolution rates are lower but the carbon capture efficiency is stable for geological timescales.

In view of more comprehensive assessments of EW efficiency, the evaluations of ACE for soils, lakes and oceans, provide the necessary benchmarks for the quantification of EW efficiency in terms of inorganic carbon sequestered in the water. In particular, the results reveal the importance of hydrological connectivity for EW and call for developing integrated biogeochemical and hydrological theories (Li et al., 2021; Regnier et al., 2022) to quantify the timescales of the mineral cation transport along the hydrological cycle and investigate the role of ecosystem uptake and soil adsorption. These theories and models will clearly need to be combined with field analysis at different spatial and temporal scales to determine the actual mineral cation transport rates and the feedbacks of the biosphere.

CRediT authorship contribution statement

Matteo B. Bertagni: Conceptualization, Methodology, Investigation, Writing – original draft, Visualization. **Amilcare Porporato:** Conceptualization, Supervision, Writing – review & editing, Funding acquisition.

Declaration of competing interest

The authors declare the following financial interests/personal relationships which may be considered as potential competing interests:

Amilcare Porporato reports financial support was provided by BP Plc. Amilcare Porporato reports financial support was provided by National Science Foundation.

Acknowledgements

We acknowledge fruitful discussions with S. Calabrese and financial support by the BP through the Carbon Mitigation Initiative (CMI) at Princeton University, the US National Science Foundation (NSF) grant nos. EAR1331846 and EAR-1338694, and the Moore Foundation.

Appendix A. Derivation of ACE

We derive the alkalization carbon-capture efficiency (ACE) starting from the definitions of dissolved inorganic carbon (DIC) and alkalinity (Alk). Alkalinity is here defined in terms of carbonates and borates, since these are the most important weak acids commonly present in natural waters (Zeebe and Wolf-Gladrow, 2001; Morel and Hering, 1993; Stumm and

Morgan, 2012). In the Supplementary Information, we report a more broad derivation of ACE accounting for the possible presence of other weak acids or bases in the alkalinity definition. We use a quasi-steady approximation, wherein the mineral dissolution is the time-limiting step, and hence consider equilibrium conditions of the water-air system.

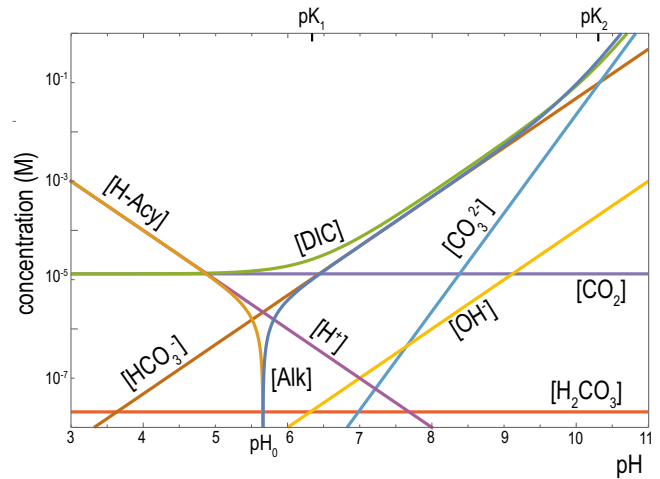


Fig. A.6. Aqueous carbonate system and alkalinity [Alk] as a function of pH for a surface freshwater in equilibrium with the atmosphere ($p_{\text{CO}_2} = 4 \cdot 10^{-4} \text{ atm}$). [H-Acy] is the mineral acidity, i.e., $[\text{H-Acy}] = -[\text{Alk}]$ when $[\text{Alk}] < 0$ (Stumm and Morgan, 2012). The pH of transition between mineral acidic ($[\text{H-Acy}] > 0$) and alkaline ($[\text{Alk}] > 0$) conditions is $\text{pH}_0 \approx 5.6$ for a surface freshwater in equilibrium with the atmosphere. Equilibrium constants are evaluated after (Stumm and Morgan, 2012) for standard conditions.

Dissolved inorganic carbon (DIC) and alkalinity (Alk) read

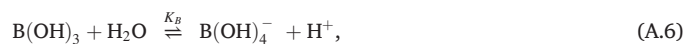
$$[\text{DIC}] = [\text{HCO}_3^-] + [\text{CO}_3^{2-}] + [\text{CO}_2], \quad (\text{A.1})$$

$$[\text{Alk}] = [\text{HCO}_3^-] + 2[\text{CO}_3^{2-}] + [\text{B(OH)}_4^-] + [\text{OH}^-] - [\text{H}^+], \quad (\text{A.2})$$

where the square brackets indicate molar concentration (M); $[\text{CO}_2]$ is the sum of carbon dioxide in aqueous form $[\text{CO}_2(\text{aq})]$ ($>99.5\%$) and the true undissociated carbonic acid $[\text{H}_2\text{CO}_3]$ ($<0.5\%$). At equilibrium, $[\text{CO}_2]$ is related to the partial pressure of carbon dioxide in the air phase (p_{CO_2}) through Henry's law

$$[\text{CO}_2] = K_H p_{\text{CO}_2}, \quad (\text{A.3})$$

where K_H is Henry's solubility constant (M/atm). The ions in (A.1) and (A.2) arise from the reactions



where K 's are equilibrium constants (evaluated after (Stumm and Morgan, 2012) for freshwater and (Zeebe and Wolf-Gladrow, 2001) for seawater). All quantities in the aqueous system above can be expressed analytically in terms of only two components; choosing p_{CO_2} and pH ($\text{pH} = -\text{Log}[\text{H}^+]$) as independent variables, one can write [DIC] and [Alk] as (Zeebe and Wolf-Gladrow, 2001; Morel and Hering, 1993; Stumm and Morgan, 2012).

$$[\text{DIC}] = K_H p_{\text{CO}_2} \left(1 + \frac{K_1}{[\text{H}^+]} + \frac{K_1 K_2}{[\text{H}^+]^2} \right),$$

$$[\text{Alk}] = \frac{K_1 K_H p_{\text{CO}_2}}{[\text{H}^+]} + \frac{2K_1 K_2 K_H p_{\text{CO}_2}}{[\text{H}^+]^2} + \dots$$

$$\dots \frac{[\text{B}_T] K_B}{[\text{H}^+] + K_B} + \frac{K_w}{[\text{H}^+]} - [\text{H}^+],$$

where $[\text{B}_T]$ is the total boron concentration, which is related to seawater salinity (S) through $[\text{B}_T] = 4.16 \cdot 10^{-4} S/35$ (M) (Zeebe and Wolf-Gladrow, 2001). $[\text{B}_T] \approx 0$ in freshwaters. We can then evaluate $[\text{DIC}]$ and $[\text{Alk}]$ differentials with respect to a variation in $[\text{H}^+]$ (constant p_{CO_2}) as

$$d[\text{DIC}] = \frac{\partial[\text{DIC}]}{\partial[\text{H}^+]} d[\text{H}^+], \quad d[\text{Alk}] = \frac{\partial[\text{Alk}]}{\partial[\text{H}^+]} d[\text{H}^+], \quad (\text{A.7})$$

where $\partial \cdot / \partial \cdot$ indicates partial differentiation and

$$\frac{\partial[\text{DIC}]}{\partial[\text{H}^+]} = - \frac{K_1 K_H p_{\text{CO}_2} ([\text{H}^+] + 2K_2)}{[\text{H}^+]^3}, \quad (\text{A.8})$$

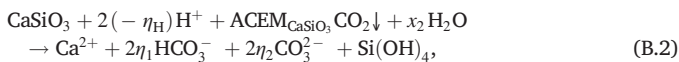
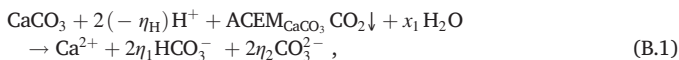
$$\frac{\partial[\text{Alk}]}{\partial[\text{H}^+]} = - \frac{k p_{\text{CO}_2} + [\text{H}^+] (K_1 K_H p_{\text{CO}_2} + K_w) + [\text{H}^+]^3}{[\text{H}^+]^3} - f_B. \quad (\text{A.9})$$

Further taking the ratio of the two differentials yields the sought measure of efficiency, i.e., Eq. (5) in the main text. The contributions of borates to ACE for seawater reads

$$f_B = \frac{K_B}{([\text{H}^+] + K_B)^2} [\text{B}_T]. \quad (\text{A.10})$$

Appendix B. Fractional reaction equations

As exemplified by the reactions (1)–(4), the dissolution of a mineral can lead to different reaction products depending on the water chemistry where the dissolution occurs. In particular, the two cases represented by (1)–(2) and (3)–(4) for CaCO_3 and CaSiO_3 dissolution are the two end members along a continuum of water-chemistry conditions that correspond to different alkalization carbon-capture efficiencies. It is possible to account for this water-chemistry continuum by writing the dissolution equations with variable coefficients as (Hofmann et al., 2010)



where $x_1 = \eta_1 + \eta_H$ and $x_2 = \eta_1 + \eta_H + 2$. Hofmann (Hofmann et al., 2010) referred to this type of equations as *fractional reaction equations*, because the stoichiometric coefficients are usually fractions, as opposed to the *integer reaction equations*, like (1)–(4), where the stoichiometric coefficients are integer.

Theoretically, (B.1)–(B.2) provide an infinite number of possibilities to write the mineral dissolution equations that are all stoichiometrically correct, provided that the mass balances of the different elements are satisfied. However, only certain sets of the stoichiometric coefficients have chemical meaning. These coefficients are in fact defined by the specific response of the aqueous carbonate species of interest to the small alkalinity addition by the mineral dissolution. Hence, as done for ACE derivation, we can define

$$\eta_1 = \frac{d[\text{HCO}_3^-]}{d[\text{Alk}]} = \frac{K_1 K_H p_{\text{CO}_2} [\text{H}^+]}{k p_{\text{CO}_2} + [\text{H}^+] (K_1 K_H p_{\text{CO}_2} + K_w) + [\text{H}^+]^3}, \quad (\text{B.3})$$

$$\eta_2 = \frac{d[\text{CO}_3^{2-}]}{d[\text{Alk}]} = \frac{2K_1 K_2 K_H p_{\text{CO}_2}}{k p_{\text{CO}_2} + [\text{H}^+] (K_1 K_H p_{\text{CO}_2} + K_w) + [\text{H}^+]^3}, \quad (\text{B.4})$$

$$\eta_H = \frac{d[\text{H}^+]}{d[\text{Alk}]} = - \frac{[\text{H}^+]^3}{k p_{\text{CO}_2} + [\text{H}^+] (K_1 K_H p_{\text{CO}_2} + K_w) + [\text{H}^+]^3}, \quad (\text{B.5})$$

where the formulas are reported for freshwater ($[\text{B}_T] \approx 0$). Note that the variation in $[\text{OH}^-]$ is not reported because it is always negligible.

Fig. C.7 shows how η_1 , η_2 and η_H vary as a function of the water pH. When the water is acidic ($\text{pH} < 5$), the alkalinity addition consumes acidity ($\eta_H \approx -1$) and does not promote aqueous carbonate formation ($\eta_1 \approx \eta_2 \approx 0$). Therefore, (B.1)–(B.2) reduce to (3)–(4). When the water is slightly alkaline ($6 < \text{pH} < 8$), the alkalinity addition promotes bicarbonates formation ($\eta_1 \approx 1$) and does not affect the concentration of H^+ or CO_3^{2-} ($\eta_H \approx \eta_2 \approx 0$). Therefore, (B.1)–(B.2) reduce to (1)–(2). Using the same definitions (B.3)–(B.5), it is possible to generalize the dissolution reaction of any alkaline mineral of interest.

Appendix C. Data and methods for topsoil application

To evaluate ACE in the world topsoils, we used soil pH data from (Wieder et al., 2014) and we estimated the p_{CO_2} in the soil air from data of evapotranspiration, following (Brook et al., 1983; Kessler and Harvey, 2001). Evapotranspiration is a convenient proxy for plant biomass, which in turn is correlated to the amount of soil CO_2 generated by decomposition of organic material. Global maps of soil pH and p_{CO_2} are in the Supplementary Material (Fig. S3 and S4).

To assess suitable environments for EW applications and the influence of the hydroclimatic forcings on the dissolution rate, we also used data of temperature, evapotranspiration, rainfall, soil moisture and potential evapotranspiration that are 2000–2020 averages from the Global Land Data Assimilation System (Rodell et al., 2004).

Following (Lasaga, 1984; Cipolla et al., 2021), we considered that the mineral dissolution rates scale with temperature, soil moisture and pH as

$$r \propto s [\text{H}^+]^\theta \exp(-E/RT), \quad (\text{C.1})$$

where s is the time-averaged relative soil moisture. Temperature affects the dissolution rate through an Arrhenius equation, where $A = 60$ kJ/mol is the mean activation energy and $R = 8.31$ J/(mol K) is the ideal gas constant (Lasaga, 1984). The activity of the hydrogen ion is approximated with its concentration ($\theta = 1$). The results for Fig. 3b are then normalized by introducing the proportionality constant r_0 so that $\min(r/r_0) = 1$. The biotic influence on the mineral dissolution rate (Vicca et al., 2022) is only considered through the abiotic drivers soil moisture and temperature.

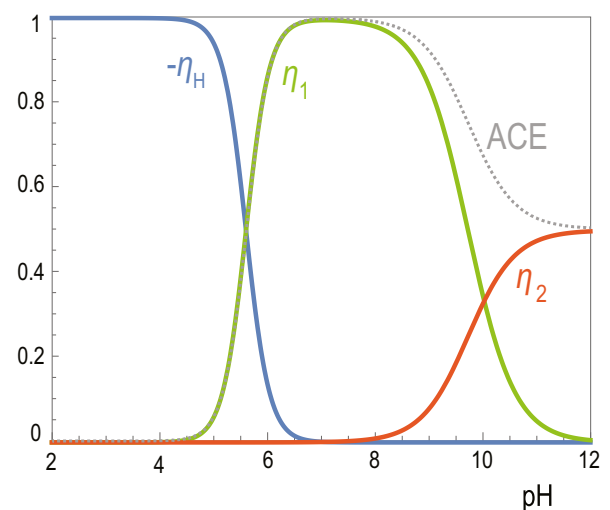


Fig. C.7. Variation of $[\text{H}^+]$, $[\text{HCO}_3^-]$, $[\text{CO}_3^{2-}]$ due to a small alkalinity addition as a function of pH (freshwater, atmospheric p_{CO_2}). Note that η_H is reported with opposite sign (added alkalinity consumes H^+) and that $\text{ACE} = \eta_1 + \eta_2$.

References

- Griscom, B.W., Adams, J., Ellis, P.W., Houghton, R.A., Lomax, G., Miteva, D.A., Schlesinger, W.H., Shoch, D., Siikamäki, J.V., Smith, P., et al., 2017. Natural climate solutions. *Proc. Natl. Acad. Sci.* 114, 11645–11650.
- Palaca, S., Al-Kaisi, M., Barteau, M., Belmont, E., Benson, S., Birdsey, R., Boysen, D., Duren, R., Hopkinson, C., Jones, C., 2018. Negative Emissions Technologies and Reliable Sequestration: A Research Agenda.
- Beerling, D.J., Kantzas, E.P., Lomas, M.R., Wade, P., Eufrazio, R.M., Renforth, P., Sarkar, B., Andrews, M.G., James, R.H., Pearce, C.R., et al., 2020. Potential for large-scale CO₂ removal via enhanced rock weathering with croplands. *Nature* 583, 242–248.
- Köhler, P., Hartmann, J., Wolf-Gladrow, D.A., 2010. Geoengineering potential of artificially enhanced silicate weathering of olivine. *Proc. Natl. Acad. Sci.* 107, 20228–20233.
- Calabrese, S., Wild, B., Bertagni, M.B., Bourg, I.C., White, C., Cipolla, G., Noto, L.V., Porporato, A., 2022. Nano- to Global-scale Uncertainties in Terrestrial Enhanced Weathering Under Review.
- Hartmann, J., West, A.J., Renforth, P., Köhler, P., De La Rocha, C.L., Wolf-Gladrow, D.A., Dürr, H.H., Scheffran, J., 2013. Enhanced chemical weathering as a geoengineering strategy to reduce atmospheric carbon dioxide, supply nutrients, and mitigate ocean acidification. *Rev. Geophys.* 51, 113–149.
- Calabrese, S., Porporato, A., 2020. Wetness controls on global chemical weathering. *Environ. Res. Commun.* 2 (8), 085005.
- Beerling, D.J., Leake, J.R., Long, S.P., Scholes, J.D., Ton, J., Nelson, P.N., Bird, M., Kantzas, E., Taylor, L.L., Sarkar, B., et al., 2018. Farming with crops and rocks to address global climate, food and soil security. *Nat. Plants* 4, 138–147.
- Goll, D.S., Ciais, P., Amann, T., Buermann, W., Chang, J., Eker, S., Hartmann, J., Janssens, I., Li, W., Obersteiner, M., et al., 2021. Potential CO₂ removal from enhanced weathering by ecosystem responses to powdered rock. *Nat. Geosci.* 14, 545–549.
- Renforth, P., Henderson, G., 2017. Assessing Ocean alkalinity for carbon sequestration. *Rev. Geophys.* 55, 636–674.
- Haque, F., Chiang, Y.W., Santos, R.M., 2020. Risk assessment of ni, cr, and si release from alkaline minerals during enhanced weathering. *Open Agric.* 5, 166–175.
- West, T.O., McBride, A.C., 2005. The contribution of agricultural lime to carbon dioxide emissions in the United States: dissolution, transport, and net emissions. *Agric. Ecosyst. Environ.* 108, 145–154.
- Klein, C., De Novoa, R., Ogle, S., Smith, K., Rochette, P., Wirth, T., McConkey, B., Mosier, A., Rypdal, K., 2006. IPCC guidelines for national greenhouse gas inventories, volume 4, chapter 11: N₂O emissions from managed soils, and CO₂ emissions from lime and urea application. Technical Report. Technical Report 4-88788-032-4, Intergovernmental Panel on Climate Change.
- Hamilton, S.K., Kurzman, A.L., Arango, C., Jin, L., Robertson, G.P., 2007. Evidence for carbon sequestration by agricultural liming. *Glob. Biogeochem. Cycles* 21.
- Wang, Y., Yao, Z., Zhan, Y., Zheng, X., Zhou, M., Yan, G., Wang, L., Werner, C., Butterbach-Bahl, K., 2021. Potential benefits of liming to acid soils on climate change mitigation and food security. *Glob. Chang. Biol.* 27 (12), 2807–2821.
- Frankignoulle, M., 1994. A complete set of buffer factors for acid/base CO₂ system in seawater. *J. Mar. Syst.* 5, 111–118.
- Egleston, E.S., Sabine, C.L., Morel, F.M., 2010. Revelle revisited: buffer factors that quantify the response of ocean chemistry to changes in DIC and alkalinity. *Glob. Biogeochem. Cycles* 24.
- Humphreys, M.P., Daniels, C.J., Wolf-Gladrow, D.A., Tyrrell, T., Achterberg, E.P., 2018. On the influence of marine biogeochemical processes over CO₂ exchange between the atmosphere and ocean. *Mar. Chem.* 199, 1–11.
- Middelburg, J.J., Soetaert, K., Hagens, M., 2020. Ocean alkalinity, buffering and biogeochemical processes. *Rev. Geophys.* 58, e2019RG000681.
- Revelle, R., Suess, H.E., 1957. Carbon dioxide exchange between atmosphere and ocean and the question of an increase of atmospheric CO₂ during the past decades. *Tellus* 9, 18–27.
- Zeebe, R.E., Wolf-Gladrow, D., 2001. CO₂ in Seawater: Equilibrium, Kinetics, Isotopes. 65. Gulf Professional Publishing.
- Wolf-Gladrow, D.A., Zeebe, R.E., Klaas, C., Körtzinger, A., Dickson, A.G., 2007. Total alkalinity: the explicit conservative expression and its application to biogeochemical processes. *Mar. Chem.* 106, 287–300.
- Renforth, P., 2019. The negative emission potential of alkaline materials. *Nat. Commun.* 10, 1–8.
- Kheshgi, H.S., 1995. Sequestering atmospheric carbon dioxide by increasing ocean alkalinity. *Energy* 20, 915–922.
- Amann, T., Hartmann, J., Struyf, E., Garcia, W.D., Oliveira, Fischer, E.K., Janssens, I., Meire, P., Schoelynck, J., 2020. Enhanced weathering and related element fluxes—a cropland mesocosm approach. *Biogeosciences* 17, 103–119.
- EPA, 2021. EPA Long-term Monitoring of Acidified Surface Waters.
- Clair, T.A., Dennis, I.F., Vet, R., 2011. Water chemistry and dissolved organic carbon trends in lakes from Canada's Atlantic provinces: no recovery from acidification measured after 25 years of lake monitoring. *Can. J. Fish. Aquat. Sci.* 68, 663–674.
- Taylor, L.L., Driscoll, C.T., Groffman, P.M., Rau, G.H., Blum, J.D., Beerling, D.J., 2021. Increased carbon capture by a silicate-treated forested watershed affected by acid deposition. *Biogeosciences* 18, 169–188.
- Kelland, M.E., Wade, P.W., Lewis, A.L., Taylor, L.L., Sarkar, B., Andrews, M.G., Lomas, M.R., Cotton, T.A., Kemp, S.J., James, R.H., et al., 2020. Increased yield and CO₂ sequestration potential with the C4 cereal sorghum bicolor cultivated in basaltic rock dust-amended agricultural soil. *Glob. Chang. Biol.* 26, 3658–3676.
- Lewis, E., Wallace, D., 1998. Program Developed for CO₂ System Calculations, Technical Report. Environmental System Science Data Infrastructure for a Virtual Ecosystem.
- Olsen, A., Lange, N., Key, R.M., Tanhua, T., Álvarez, M., Becker, S., Bittig, H.C., Carter, B.R., da Cunha, L., Cotrim, Feely, R.A., 2019. Glodapv2. 2019—an update of glodapv2. *Earth Syst. Sci. Data* 11, 1437–1461.
- Olsen, A., Lange, N., Key, R.M., Tanhua, T., Bittig, H.C., Kozyr, A., Álvarez, M., Azetsu-Scott, K., Becker, S., Brown, P.J., 2020. Glodapv2. 2020—the second update of glodapv2. *Earth Syst. Sci. Data* 165.
- Locarnini, M., Mishonov, A., Baranova, O., Boyer, T., Zweng, M., Garcia, H., Seidov, D., Weathers, K., Paver, C., Smolyar, I., 2018. World ocean atlas 2018. Temperature 1.
- Zweng, M., Seidov, D., Boyer, T., Locarnini, M., Garcia, H., Mishonov, A., Baranova, O., Weathers, K., Paver, C., Smolyar, I., 2019. World ocean atlas 2018. Salinity 2.
- Mant, R.C., Jones, D.L., Reynolds, B., Ormerod, S.J., Pullin, A.S., 2013. A systematic review of the effectiveness of liming to mitigate impacts of river acidification on fish and macroinvertebrates. *Environ. Pollut.* 179, 285–293.
- Menz, F.C., Seip, H.M., 2004. Acid rain in Europe and the United States: an update. *Environ. Sci. Pol.* 7, 253–265.
- Sterling, S., Angelidis, C., Armstrong, M., Biagi, K., Clair, T., Jackson, N., Breen, A., 2014. Terrestrial liming to promote Atlantic salmon recovery in Nova Scotia—approaches needed and knowledge gained after a trial application. *Hydrol. Earth Syst. Sci. Discuss.* 11, 10117–10156.
- Covino, T., 2017. Hydrologic connectivity as a framework for understanding biogeochemical flux through watersheds and along fluvial networks. *Geomorphology* 277, 133–144.
- Gattuso, J.-P., Hansson, L., 2011. Ocean Acidification. Oxford University Press.
- Gruber, N., Clement, D., Carter, B.R., Feely, R.A., Heuven, S.V., Hoppema, M., Ishii, M., Key, R.M., Kozyr, A., Lauvset, S.K., 2019. The oceanic sink for anthropogenic CO₂ from 1994 to 2007. *Science* 363, 1193–1199.
- Mongin, M., Baird, M.E., Lenton, A., Neill, C., Akl, J., 2021. Reversing ocean acidification along the Great Barrier Reef using alkalinity injection. *Environ. Res. Lett.* 16, 064068.
- Li, L., Sullivan, P.L., Benettin, P., Cirpka, O.A., Bishop, K., Brantley, S.L., Knapp, J.L., van Meerveld, I., Rinaldo, A., Seibert, J., et al., 2021. Toward catchment hydrobiogeochemical theories. *Wiley Interdiscip. Rev. Water* 8, e1495.
- Regnier, P., Resplandy, L., Najjar, R.G., Ciais, P., 2022. The land-to-ocean loops of the global carbon cycle. *Nature* 603, 401–410.
- Morel, F.M., Hering, J.G., 1993. Principles and Applications of Aquatic Chemistry. John Wiley & Sons.
- Stumm, W., Morgan, J.J., 2012. Aquatic Chemistry: Chemical Equilibria and Rates in Natural Waters. volume 126. John Wiley & Sons.
- Hofmann, A., Middelburg, J., Soetaert, K., Wolf-Gladrow, D., Meysman, F., 2010. Proton cycling, buffering, and reaction stoichiometry in natural waters. *Mar. Chem.* 121, 246–255.
- Wieder, W., Boehner, J., Bonan, G., Langseth, M., 2014. RegridDED harmonized world soil database v1. 2. ORNL DAAC.
- Brook, G.A., Folkoff, M.E., Box, E.O., 1983. A world model of soil carbon dioxide. *Earth Surf. Process. Landf.* 8, 79–88.
- Kessler, T.J., Harvey, C.F., 2001. The global flux of carbon dioxide into groundwater. *Geophys. Res. Lett.* 28, 279–282.
- Rodell, M., Houser, P., Jambor, U., Gottschalk, J., Mitchell, K., Meng, C.-J., Arsenault, K., Cosgrove, B., Radakovich, J., Bosilovich, M., et al., 2004. The global land data assimilation system. *Bull. Am. Meteorol. Soc.* 85, 381–394.
- Lasaga, A.C., 1984. Chemical kinetics of water-rock interactions. *J. Geophys. Res. Solid Earth* 89, 4009–4025.
- Cipolla, G., Calabrese, S., Noto, L.V., Porporato, A., 2021. The role of hydrology on enhanced weathering for carbon sequestration I. Modeling rock-dissolution reactions coupled to plant, soil moisture, and carbon dynamics. *Adv. Water Resour.* 154, 103934.
- Vicca, S., Goll, D.S., Hagens, M., Hartmann, J., Janssens, I.A., Neubeck, A., Peñuelas, J., Poblador, S., Rijnders, J., Sardans, J., et al., 2022. Is the climate change mitigation effect of enhanced silicate weathering governed by biological processes? *Glob. Chang. Biol.* 28, 711–726.